

Electrodynamics of the Getaway Tether Experiment

Michael Greene*

Auburn University, Auburn, Alabama

Douglas Wheelock†

SCI Systems, Huntsville, Alabama

and

Michael Baginski‡

Auburn University, Auburn, Alabama

An electrodynamic circuit model of the interaction of a pair of small tethered satellites and the ionosphere is developed and analyzed. The system under study, the Getaway Tether Experiment (GATE), is composed of two small satellites and 1 km of insulated conducting tether. The nonlinear model has elements representing the emission, collection, and resistive flow of charge through an electrically conductive tether, plasma contactors, and the ionosphere. The circuit model is incorporated into a dynamic orbital simulation to predict mission performance. Simulation results show the feasibility to bilaterally transfer energy between stored electrical energy and orbital momentum. A transient model is also developed using the circuit model and a string of N lumped-parameter modules, each consisting of resistance, capacitance, and induced potential for the tether. Transients are shown via simulation to occur over millisecond intervals.

Nomenclature

A_M	= surface area of mother	V_c	= mother subsatellite potential
A_f	= filament surface area	v	= velocity vector
B	= magnetic field vector	v_{the}	= electron thermal velocity
B_h	= horizontal components of B	v_{thi}	= ion thermal velocity
B_v	= vertical components of B	α	= proportionality factor
B_0	= 0.45 G	β	= resistance temperature coefficient
C	= capacitance of mother	δ	= probe potential
C_k	= capacitance of tether segment	δ_f	= filament work function
D	= Debye shielding distance	ϵ_0	= free space permittivity
e	= electronic charge	η	= normalized potential
I	= current	θ	= magnetic colatitude
I_0	= net current at zero potential	μ	= gravitational constant
i	= orbital inclination	ω	= electron gyroresonant frequency
J_0	= current density at zero potential	ω_E	= Earth rotational frequency
K	= 120 A/cm ² K ²	ω_G	= Getaway Tether Experiment orbital frequency
k	= Boltzmann's constant		
L	= tether length vector		
l_m	= mean free path of particles		
m	= mass		
N	= number of tether segments		
N_e, N_i	= electron and ion density		
R_E	= radius of the Earth		
R_L	= load resistance		
R_T	= tether resistance		
R_k	= resistance of tether segment		
R_0/R_1	= inner/outer radius of plasma sheath		
r_f	= filament radius		
T	= temperature		
V_E	= emitter potential		
V_a	= applied voltage source		

Introduction

ONE of the most convenient methods for satellite deployment from the Space Shuttle is the "Getaway Special" (GAS), a system that requires only a release command from the Orbiter. The Getaway Tether Experiment (GATE), described in recent papers,¹⁻³ is a low-cost tethered satellite system that may be released from the GAS canister into a low-Earth orbit. The GATE consists of two subsatellites connected by an insulated, conducting tether. The orbit of the GATE will carry it through the lower F region of the ionosphere, an appropriate setting for experiments in an anisotropic, magnetized plasma. Since the early 1960's, researchers have examined the characteristics of a tethered satellite system in low-Earth orbit, and the GATE could be one of the first demonstrations of this technology.

One motivation for the GATE is the length of its proposed mission life: GATE will orbit the Earth for eight or more weeks, relaying the data collected from electrodynamic experiments to ground stations every orbit, whereas experiments with sounding rockets have a very short mission length covering many layers of the ionosphere. GATE can map the plasma-tether characteristics over many orbits, aiding in the design of future experiments and demonstrating the dynamic exchange between orbital and stored electrical energy.

Received Feb. 2, 1988; revision received March 24, 1989. Copyright © 1989 American Institute of Aeronautics and Astronautics, Inc. All rights reserved.

*Associate Professor, Department of Electrical Engineering.

†Engineer.

‡Assistant Professor, Department of Electrical Engineering.

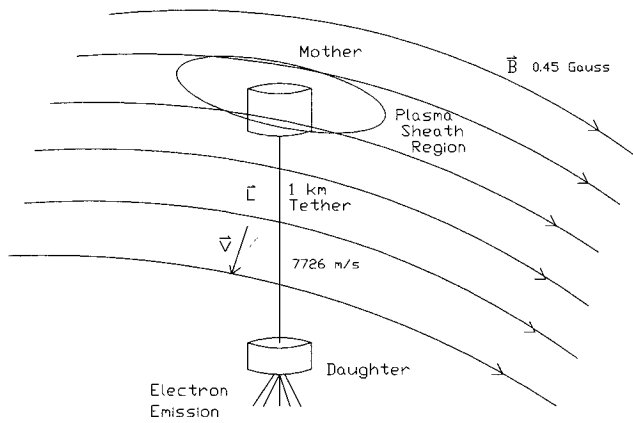


Fig. 1 Getaway Tether Experiment: magnetic field strength is approximately 0.45 g, and the orbital velocity is 7726 m/s.

As shown in Fig. 1, the system consists of "mother" and "daughter" subsatellites connected by a flexible tether. Both subsatellites are cylindrical with a diameter of 0.46 m, but the daughter displaces approximately one-third the volume of the mother. The mother passively contacts the plasma, while the daughter does so actively with either an electron emitter or a hollow cathode device. A braided, flexible, insulated cable with a diameter of approximately 1–2 mm and nominal length of 1000 m connects the mother and daughter subsatellites. The tether has an electrically conductive path with the characteristic of an insulated copper wire. The electrical connection between the tether, subsatellite, and plasma will be controlled by internal electronics. An insulated conductive tether was chosen to minimize the loss of electrons to the surrounding plasma.⁴

In this study, the system orbits at an altitude of 300 km with a velocity of approximately 7726 m/s. The motion of the electrodynamic tether through the geomagnetic field results in an electromotive force $\mathbf{v} \times \mathbf{B}$ along its length. For a nominal magnetic field strength of 0.45 G and nominal length of 1000 m, this electromotive force (emf) causes a potential drop of approximately 350 V across the tether. This paper will show that when the subsatellites of GATE complete an electrical circuit between the tether and the plasma, a current on the order of tens to hundreds of milliamperes results. The passage of this current through the electrodynamic tether causes the Lorentz force $I\mathbf{L} \times \mathbf{B}$ to accelerate the system and thus alter its orbit. Assuming eastward orbital motion and an Earth-centered coordinate system, the current in the tether is directed upward, and the $I\mathbf{L} \times \mathbf{B}$ force opposes the velocity of the system. It will be shown that for sufficient opposing emf, the current direction in the tether may be reversed, resulting in an acceleration in the same direction as the velocity of the satellite pair.

Electrodynamic Circuit Model

The steady-state electrodynamic circuit model of GATE is shown in Fig. 2. Inserted between the tether resistance R_T and the current source I_C is a voltage source and a series resistance. Assuming eastward motion of the system and $V_a = 0$, current is directed up the tether, the polarity of the emf in Fig. 2 is positive, and the current I performs useful work in load resistance R_L . The system in this configuration is in the "charging mode." Useful work such as charging batteries is done at the expense of orbital momentum, and the rate of change of orbital energy is $\text{emf} \times I$. When $V_a > \text{emf}$ and R_L is the output resistance of a switching dc power supply, the net current is directed downward relative to the surface of the Earth, causing an electrodynamic force to accelerate the GATE in the same direction as its velocity. This configuration

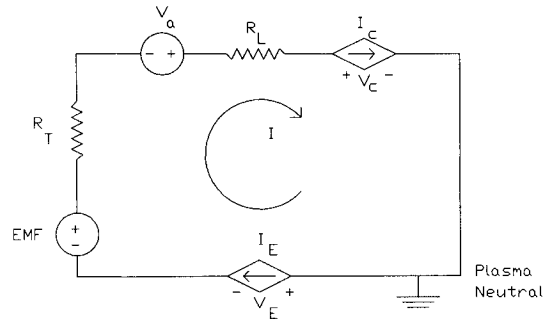


Fig. 2 GATE electrodynamic equivalent circuit.

is the "electroboost" mode. Electrical energy from storage devices is expended to increase the altitude of the satellite pair.

Another possible phenomenon that may contribute to the tether's orbital decay is that caused by Alfvén waves (electromagnetic radiation) associated with the presence of motionally induced ac currents (passive). This phenomenon has been considered in detail by Hastings et al.⁵ and Barnett and Olbert,⁶ who have characterized a system's energy loss due to radiation for low-Earth orbits. In both of the aforementioned analyses, the authors do not claim a precise calculation of the energy loss, but rather point out some of the possible effects Alfvén waves may have on orbiting conducting bodies.

For the purposes of this study, the influence Alfvén waves could have on the net energy loss relative to the specific tether experiment addressed here has been considered. It is beyond the scope of this paper to elaborate on all of the possibilities for energy loss of an orbiting system (electromagnetic or other), and only some general observations relative to the Alfvén-wave phenomenon will be stated at this time.

The major consideration regarding this energy-loss mechanism is how the resulting force is exerted on the tether. When radiation due to ac currents is present, the ac currents induce a Lorentz force aligned with the direction of orbit. Assuming that only ac currents are considered and that the possible changes in orbital velocity for time constants associated with the lowest ac frequency are negligible, it may be concluded that the net force affecting the tether's orbit is approximately zero. Admittedly, there are second-order effects possible. However, within the confines and purpose of this paper, it is considered sufficient to state the ac currents on the tether system stemming from Alfvén wave phenomenon may be an important factor, but will not be incorporated in the system studies presented here. The final determination of what the dominant energy-loss mechanisms are relative to the orbiting tether will be obtained from instrumentation when it is in orbit.

Transient-Model Development

A transient-response model has been chosen for the tether following the logic of Arnold and Dobrowolny.⁷ This model uses all the elements of Fig. 2. The remaining elements of the transient-analysis model are the capacitance of the mother subsatellite surface and the typical tether segment. The approximation of the capacitance of the mother subsatellite is a function of the radius of the smallest spherical shell enclosing the mother subsatellite R_0 and the radius of the sheath surrounding the mother subsatellite⁷ R_1 .

$$C = \frac{4\pi\epsilon_0 R_0 R_1}{R_1 - R_0} \quad (1)$$

For neutral potential relative to the plasma, the difference $R_1 - R_0$ will be assumed to be the Debye shielding distance,⁸ typically 0.5 cm for the ionosphere around the GATE. At

large absolute subsatellite potential, the radius of the sheath increases in a manner derived by Al'pert^{1,9}:

$$R_1/R_0 = 0.8 [e |V| / kT (D/R_0)^{4/3}] \quad (2)$$

If it is assumed that this model holds for both positive and negative subsatellite potential, a slight modification to this equation provides continuity with the neutral potential sheath thickness, namely,

$$R_1 = R_0 \cdot [1 + 0.8 [e |V| / kT (D/R_0)^{4/3}]] + D \quad (3)$$

At zero potential, Eq. (3) predicts a sheath radius greater than R_0 by the Debye length. In the limit of large potential, Eq. (3) closely matches the Al'pert model of Eq. (2).

The lumped-RC model of the GATE tether has a typical segment shown in Fig. 3. Let the number of tether segments be N : E_k is the Alfvén emf divided by N , and R_k is the tether resistance divided by N . The capacitance per unit length is given by⁶

$$C = 2\pi\epsilon_0/\ln(r_s/r_c) \quad (4)$$

The capacitance of the tether segment C_k is just the tether capacitance of Eq. (4) multiplied by the length of the tether divided by N .

If the current entering the right arm of the segment model is denoted IB_k and the current leaving the left arm of the segment model denoted IA_k , then the nodal tether segment potential Z_k is found as

$$dZ_k/dt = (IB_k - IA_k)/C_k \quad (5)$$

The current through the typical tether segment is a function of the potential of the ends of the segment:

$$IA_k = (Z_k + E_{k+1} - Z_{k+1})/R_k \quad (6)$$

and

$$IB_k = IA_{k-1} \quad (7)$$

Using this convention, the current through the right arm of the tether segment connected to the daughter is $IB_1 = I_c$. Because of the control electronics that can alter the series resistance of the system by R_a , the tether segment connected to the mother requires special treatment, implying

$$dV_c/dt \equiv dZ_{N+1}/dt = (IA_N - I_c)/C_m \quad (8)$$

$$IA_N = (Z_N + V_a - Z_{N+1})/(R_k + R_a) \quad (9)$$

Induced EMF

The motion of the electrodynamic tether through the geomagnetic field creates a nonelectrostatic field $E = v \times B$. For an eastward motion of the tether, positively charged particles move up the tether and electrons move toward the Earth; the resulting electric field is directed downward. The electromo-

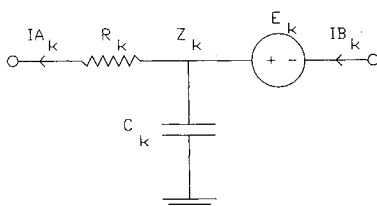


Fig. 3 Typical tether segment.

tive force developed along the length of the tether is

$$\text{emf} = \int_L v \times B \cdot d\lambda \quad (10)$$

where $d\lambda$ is directed radially outward from the Earth. GATE will employ control laws to stabilize the system along the gravity-gradient vector and minimize tether limitations. For a nominally linear tether, the electromotive force of Eq. (10) may be approximated by $\text{emf} = v \times B \cdot L$.

Electron Emission

The plasma contact characteristic of the daughter subsatellite is a nonlinear function of many variables depending on the method used. Two methods are considered for the GATE: thermionic emission and hollow cathode emission. Assuming low tether currents, thermionic emission of electrons is a function of electrode temperature and potential¹⁰:

$$I = A_f K T^2 \exp^{-(\delta_f + eV)/kT}, \quad V_0 \geq 0$$

$$I = A_f K T^2 \exp^{(-\delta_f + \sqrt{e^3 V / 4\pi e r} \beta)/kT}, \quad V < 0 \quad (11)$$

The V - I characteristic of a hollow cathode is far more complex and will be based on an empirical relationship derived from lab data of Patterson and Wilbur¹¹:

$$I = 0.03884 \exp^{-0.07541 V_e} \quad (12)$$

The plasma contact relationship of the daughter will be modeled as a voltage-dependent current source I_e connected to the distant neutral plasma.

Electron Collection

As with the daughter, the plasma contact of the mother subsatellite is a nonlinear function of many variables. From a circuit model standpoint, the skin of the mother is a voltage-dependent current source connected to a neutral area in the distant undisturbed plasma. Langmuir and Mott-Smith¹² derived explicitly the equation for current to a collector with $\eta > 0$, although their results were limited to probes in a laboratory gaseous discharge chamber. At an altitude of 300 km, the dimensions and velocity of an experiment such as the GATE are bracketed by the Debye length and mean free path of particles and the thermal velocities of ions and electrons, respectively, namely,

$$D \ll R_0 \ll l_m$$

$$v_{thi} \ll v_0 \ll v_{the} \quad (13)$$

which imply that the motion of the GATE through the plasma does not greatly disturb the velocity distribution of the electrons, and a Maxwellian drift current is appropriate. Relative to the GATE, the ionic thermal motion is minimal, and ion ram current per unit area is given by

$$J_{o,i} = \alpha N_i e v_0, \quad 0.5 < \alpha < 1.0 \quad (14)$$

Because the photoelectric emission due to solar illumination may be neglected, the charged particle flux to the surface of the subsatellites will consist of free electrons and streaming ions.¹³ For a sufficiently positive mother subsatellite surface the collected current is

$$I = A_m [N_e e \sqrt{kT/2\pi m_e} F(\delta) - \alpha N_i e v_0 \exp^{-e\delta/kT}] \quad (15a)$$

where $F(\delta)$ is a function that models the increase of electron flux in the positive sheath surrounding the mother. The corresponding equation for negative satellite potential has a con-

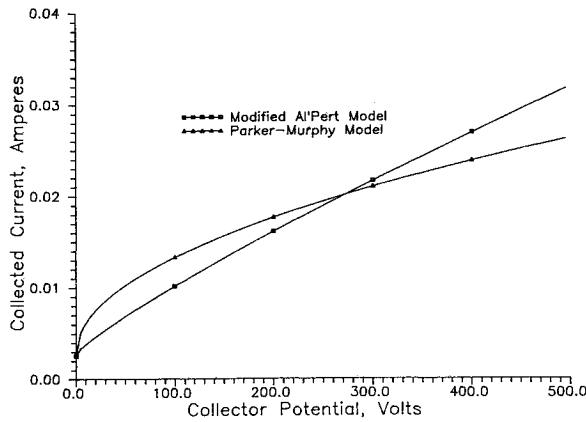


Fig. 4 Comparison of electron collection models.

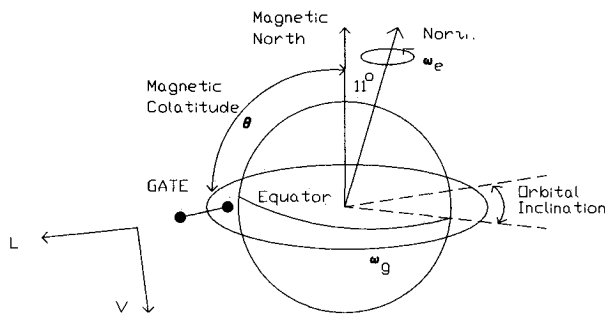


Fig. 5 GATE orbital relationships.

stant ion ram current summed with the electron current¹²:

$$I = A_m [N_e \epsilon \sqrt{kT/2\pi m_e} \exp^{-e\delta/kT} - \alpha N_i \epsilon v_0] \quad (15b)$$

The problem of finding a suitable function $F(\delta)$ for a satellite in low-Earth orbit has been considered by several authors. If the force of electrical field within the sheath dominates the magnetic forces on the motions of charged particles as confirmed by Dobrowolny and Janve,⁹ then the function $F(\delta)$ may be extracted from Al'pert et al.¹⁴ as

$$F(\delta) \equiv I/I_0 = 0.951 [(\epsilon\delta/kT)(D/r_m)^{4/3}]^{6/7} \quad (16)$$

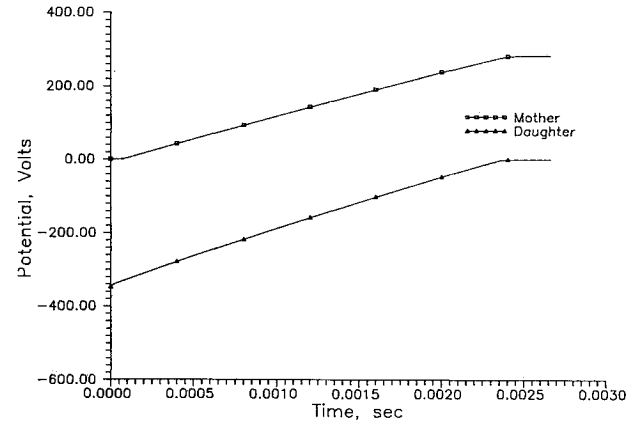
If the magnetic forces could not be so easily dismissed as contended by Parker and Murphy,¹⁵ the derivation of the function describing this electron drift mechanism follows a rigorous dynamical bounding of the sphere potential resulting in

$$F(\delta) \equiv I/I_0 \leq 1 + \sqrt{8\delta\epsilon/m_e\omega^2 r_0^2} \quad (17)$$

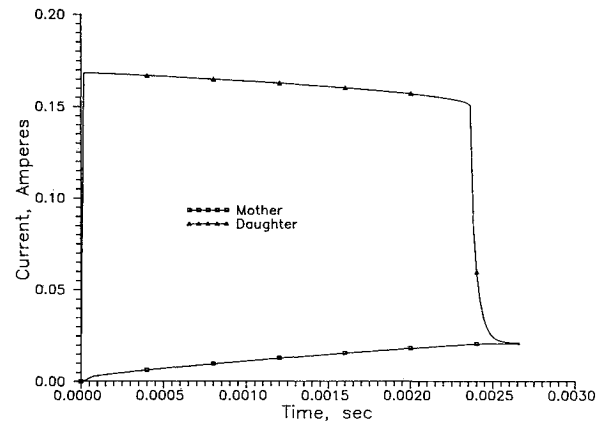
where $\omega = \epsilon B/m_e$.

Without sufficient experimental evidence, a choice between the functions $F(\delta)$ of Eqs. (16) and (17) may not be made. The equivalent electrical circuit for the GATE shown in Fig. 2 will be analyzed using these models for charged particle collection and emission. The limits of system performance may then specify requirements for the design of an electrodynamic tethered satellite system.

Figure 4 compares the $F(\delta)$ functions of Eqs. (16) and (17) for the range of satellite potential applicable to the GATE. As expected, the Al'pert model is optimistic for large potential. At low potential, however, the square root characteristic of the Parker-Murphy model exceeds the current predicted by the Al'pert model.



a) Potential



b) Current

Fig. 6 Charging mode transient response with $R_L = 3000 \Omega$.

Orbital Simulation

A simple planar orbital simulation for a point-mass with tangential thrust was adapted from Perkins.¹⁶ The equations of motion with a tangential thrust F_t are

$$\begin{aligned} r'' &= v^2/r - (r')^2/r - \mu/r^2 + F_t(r'/v) \\ v' &= F_t - (\mu/r^2)(r'/v) \end{aligned} \quad (18)$$

where μ is the gravitational constant and r is the radius from the center of the Earth. The point-mass approximation is crude, but should yield order-of-magnitude results good for early analysis. The thrust is $IL \times B$. Although electrons always will flow from mother or daughter subsatellite, the orientation of L changes between electroboost and charging modes.

An orbital simulation of the electrodynamic tether in the ionosphere requires a model for the geomagnetic field. Martinez-Sanchez and Hastings¹⁷ suggest a simple dipole model in which only the magnitude of the horizontal component of the magnetic field matters. Incorporating this model into a planar simulation yields (see Fig. 5) the following relationship between tether length, velocity, and magnetic field vector:

$$\begin{aligned} v \times B \cdot L &= v B_0 L \sin \theta (R_E/r)^3 \\ &\times \sin [1.57 - 0.192 \sin(\omega_E t) - i \cos(\omega_G t)] \end{aligned} \quad (19)$$

This electrodynamic orbital simulation will assume either a thermionic emitter or hollow cathode device at the daughter

subsattellite, and the Al'pert charged particle collection model at the mother subsattellite.

Methods

The equations for the transient model [Eqs. (1-9) and (16)] were solved iteratively using an HP 9000 computer. Numeric integrations were performed using a fourth-order Runge-Kutta algorithm. For steady-state analysis, the two nonlinear equations [Eqs. (11), or (12) and (15)], and the linear circuit equation were solved numerically. The orbital equations were solved using the fourth-order Runge-Kutta integrator.

Transient Analysis Results

Deployment and Charging

After the initial deployment sequence, the system is brought into gravity gradient orientation with the mother subsattellite above the daughter (charging mode). The skin of the mother subsattellite receives a flux of ions and electrons, but because no charged particle transfer occurs at the daughter, the tether current is zero. The potential of the mother subsattellite with respect to the neutral plasma is a small negative value, typically -0.2 V. The potential drop along the tether length is uniform, and the potential of the daughter is more negative than the mother subsattellite by $\mathbf{v} \cdot \mathbf{B} \cdot \mathbf{L}$. In the charging mode, $V_a = 0$, and the load resistance R_L is assumed to be 3000Ω .

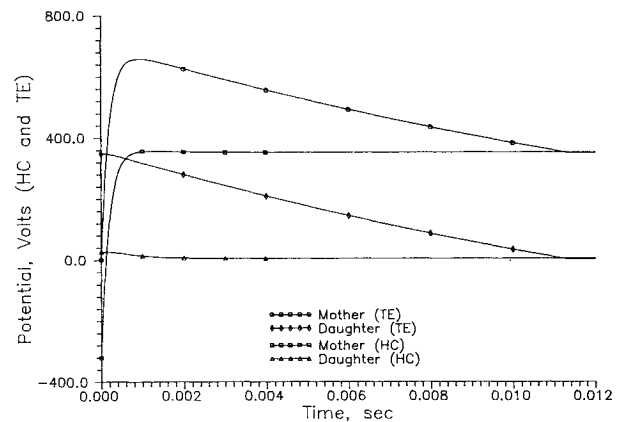
The first electrical transient occurs in the system when the daughter subsattellite begins electron emission. In order to determine the transient response time for the system, electron emission will be assumed to start abruptly as a step function. If the daughter subsattellite employs thermionic emission and the mother obeys the modified Al'pert model for charged particle collection, the typical behavior of the transient model is shown in Figs. 6a and 6b. In Fig. 6a, the potential of the daughter rises from -347.7 V toward a value slightly above the neutral plasma potential. The potential of the mother starts at the plasma potential and rises toward a maximum of $+283.7$ V. Potential drops across the tether and load prevent the mother subsattellite from attaining the $\mathbf{v} \times \mathbf{B} \cdot \mathbf{L}$ potential. In Fig. 6b, the current through the load resistor increases slowly toward the nominal value of 20.8 mA. With a negative daughter-plasma potential, the thermally emitted current remains essentially constant. Once the potential of the thermionic emitter rises above the plasma potential, the number of electrons liberated from the filament is drastically reduced. Equilibrium is reached in 2.7 ms for the nominal parameters chosen in the transient response circuit model. When the load impedance was decreased by a factor of 10, the rate of change of potential matched Fig. 6a closely. But the steady-state potential of the mother subsattellite was more positive by 55 V, whereas the steady-state current was 2 mA larger. It is interesting to note that a substantial change in load impedance has little effect on the period of the transient response in charging mode.

Electroboost

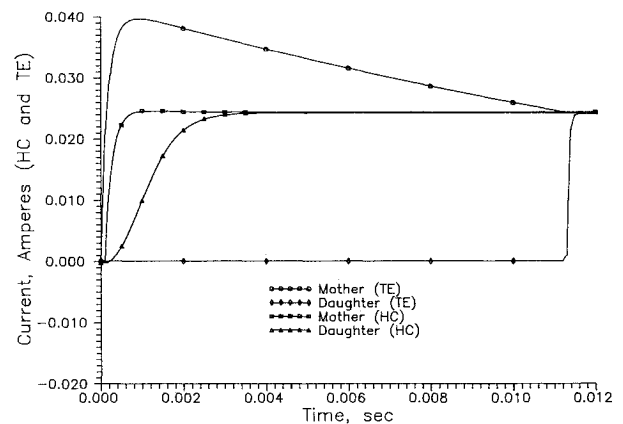
The electroboost mode can be entered by drawing the tether into the mother until angular momentum flips the orientation of the subsattellite relative to the Earth.¹ To stabilize this new orientation, the tether is played out to its nominal length again. It may be verified that the potential of the thermionic emitter is $+347.5$ V, and the potential of the mother is -0.2 V. For small potentials, the ion flux and electron flux at the mother are nearly equal, resulting in no current at the mother. Few electrons on the surface are energetic enough to escape, and the net current from the thermionic emitter is very small. Since the net current at the mother and daughter nodes of the circuit is zero, the potential difference between the subsattellites is just balanced by the induced potential. If a hollow cathode device (which can emit ions) is used as a plasma contactor in the daughter, it can be verified that the initial

tether current is -0.25 mA, and the potential of the mother and daughter are -322.08 and 25.6 V, respectively.

The mother subsattellite contains a voltage source V_a for electroboost mode, whose "on" characteristics were assumed to follow a simple exponential waveform. The time constant for this exponential characteristic was chosen to be very slow relative to the electron plasma period. As noted by Candidi et al.,¹⁸ the electron plasma frequency in low-Earth orbit ranges from 2.8 to 8.9 MHz. Therefore, a time constant of $200 \mu\text{s}$ was used for the 700 V applied potential.



a) Potential



b) Current

Fig. 7 Electroboost mode transient response: comparison between a hollow cathode contactor and a thermionic emitter.

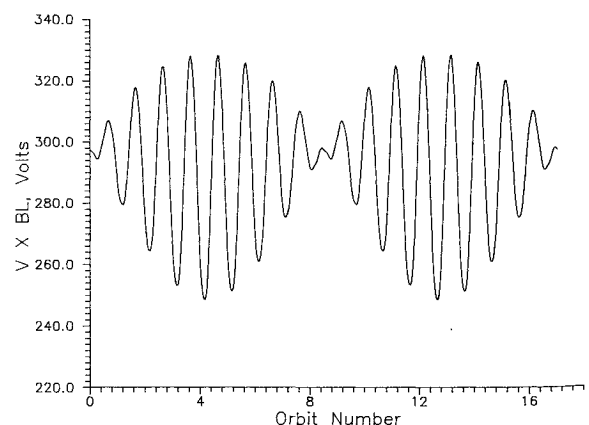


Fig. 8 Motion-induced emf during a 24-h period.

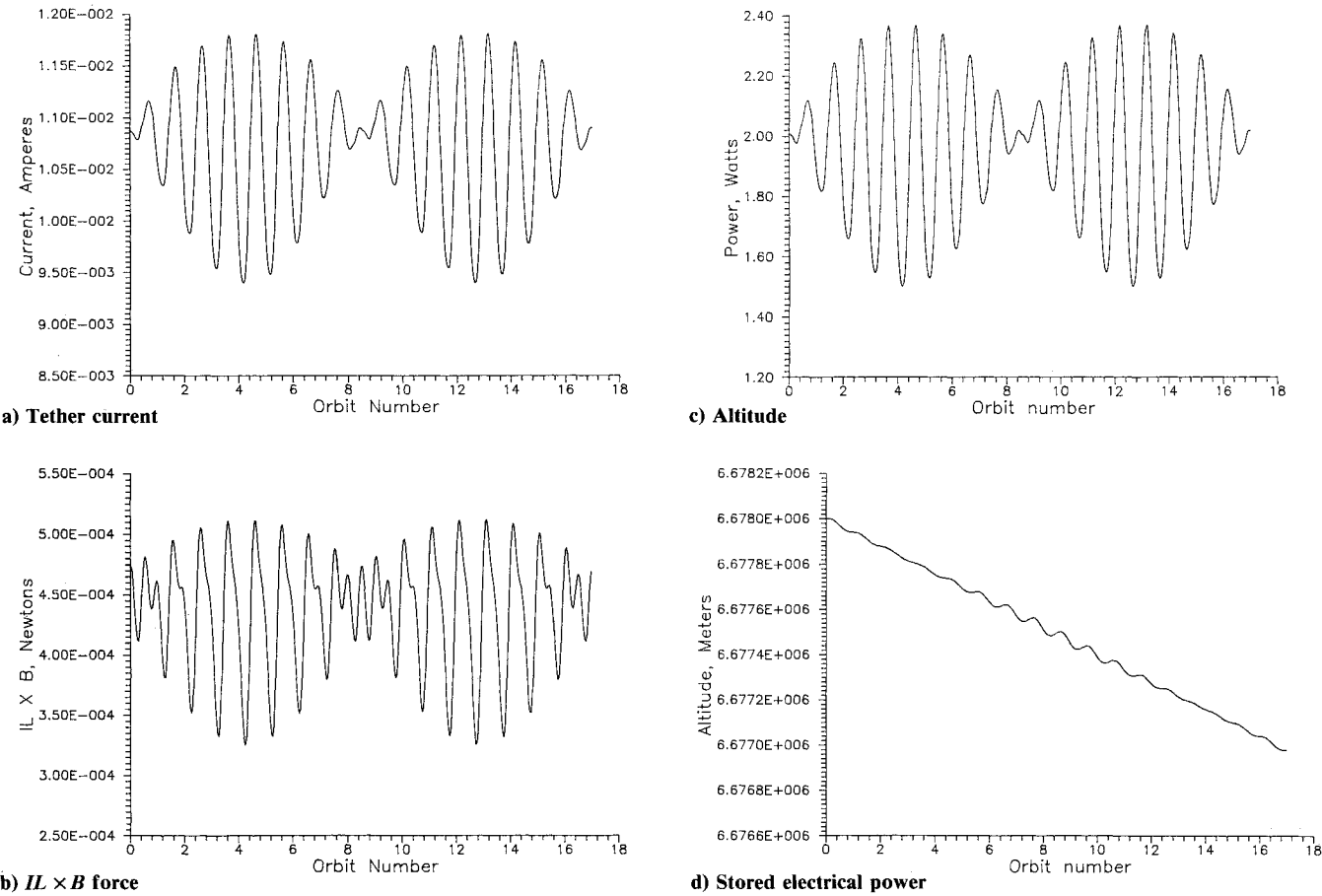


Fig. 9 Charging mode electrodynamics with Alpert collection model and thermionic emitter.

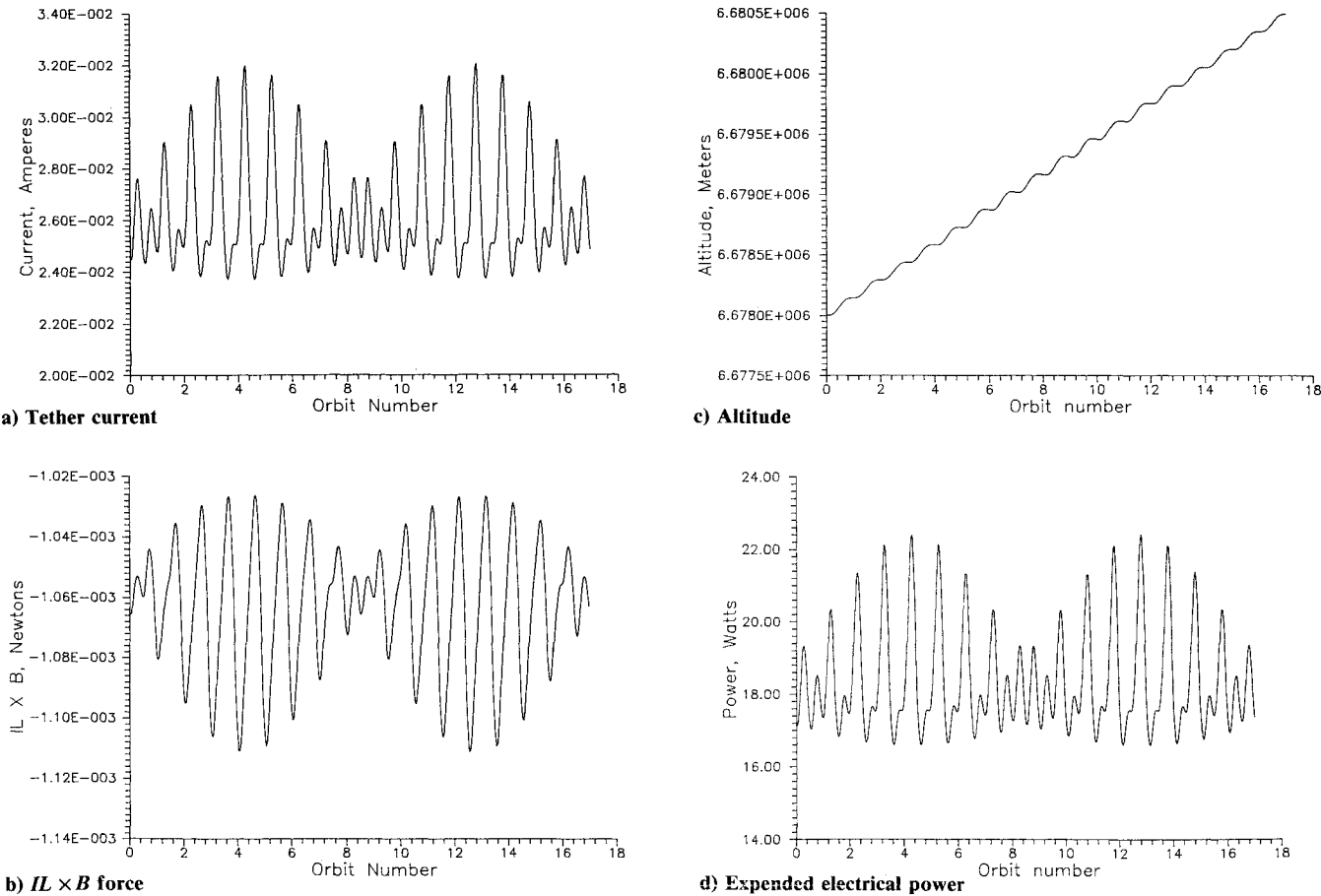


Fig. 10 Electroboost mode electrodynamics with Parker-Murphy collection model and thermionic emitter.

The transient response electroboost results are seen in Fig. 7 for the system using either a hollow cathode contactor or a thermionic emitter at the daughter. In Fig. 7a, the potential of the mother and daughter are compared for the two cases. For the thermionic case, the mother potential rises more rapidly (1-ms rise), reaches a maximum and settles to equilibrium (347 V) slowly, whereas the daughter potential gradually falls to slightly above plasma potential. For the hollow cathode case, the equilibrium (356 V) at the mother is reached in a steady but much faster rise, whereas hollow cathode falls from 25.6 V to its steady-state value of 3.35 V in only 4 ms. A comparison of the current at the two ends of the tether for the two cases is shown in Fig. 7b. For thermionic emission at the daughter, the mother current waveform follows the potential waveform and reaches a maximum value of 39.7 mA. The large positive potential of the thermionic emitter prohibits electron emission until $t = 11$ ms, when the emitted current rises rapidly to the steady-state value of 24.1 mA. The maximum power delivered from the applied voltage source is 27.6 W, and the steady-state power requirement is 16.9 W. For the hollow cathode case, the negative current in the tether is immediately reversed after the voltage source is applied. The charged particle flux rate at the mother subsatellite surface quickly rises to its equilibrium value, and the hollow cathode electron current rises to 24.3 mA after 4 ms. It is clear that less energy is expended during the transient response of the hollow cathode system as compared to the thermionic emitter system.

Steady-State Results

Figure 8 is a plot of the induced emf in a 1-km tether for an orbit with a 28 deg inclination. The primary oscillation has the same period as the orbital frequency, and the envelope varies with Earth rotation. The actual emf would be distorted from this model by anomalies in the geomagnetic field.

The results of the charging mode orbital simulation are shown in Fig. 9 using the $F(\delta)$ of Eq. (16) and a thermionic emitter. Results using a hollow cathode are essentially the same due to the current collection limitations of the mother. The charging mode tether current shown in Fig. 9a varies with the same phase as the emf curve in Fig. 8. Figure 9b shows the variations of the electrodynamic force on the tether. Because this force opposes the velocity of the GATE, the altitude of the tethered satellite system (Fig. 9c) decreases at a rate of 1 km per day. As seen in Fig. 9d, the tether current dissipates an average of 1 W into a 16-k Ω load or 24 Wh of energy per day.

The electroboost mode orbital simulation used a source voltage of 700 V, with a source resistance of 100 Ω to counteract the negative-induced emf. The results of the electroboost simulation using the $F(\delta)$ of Eq. (17) are seen in Fig. 10. Like charging mode, the electroboost current is in phase with the emf forcing function. Because the tether orientation is reversed, the phase of the current in Fig. 10a is reversed from the current in Fig. 9a, and causes the $IL \times B$ characteristic of Fig. 10b to be additive with the velocity. The gain of altitude for the electroboost simulation is drawn in Fig. 10c. At the expense of 480 Wh per day (Fig. 10d), the GATE altitude is increased 2.6 km.

Conclusions

An electrodynamic model for the Getaway Tether Experiment has been presented and simulated. Transients were shown to occur over millisecond intervals, and steady-state performance was calculated using a reduced mode with only three nonlinear equations. Although many simplifying assumptions were made, the results give a good indication of mission performance of GATE.

Several comments should be made about the result of the transient response numerical simulations. In each case, the GATE electrodynamic system started from an equilibrium state and reached a new equilibrium state in a well-behaved manner. The longest transient response lasted only 12 ms,

allowing the orbital and ionospheric parameters to be assumed constant during the transient response.

The Parker-Murphy model for electron collection was not employed in the transient response simulations due to problems determining the sheath radius as a function of potential with that model. Without this sheath radius function, the calculation of mother subsatellite capacitance makes no sense. In addition, the charging mode transient response simulation did not include the hollow cathode model for charged particle emission. The initial potential of the hollow cathode would have been -347.7 V, and the empirical volt-ampere model is not valid for potentials less than -20 V.

The transient response simulations demonstrated two important electrodynamic aspects of the GATE. In charging mode orientation, the transient response simulation showed that it is possible to raise the potential of the mother subsatellite to a large positive value above the neutral plasma potential and increase the current in the tether. In electroboost mode orientation, the motion-induced emf is reversed in the tether, and the current trends to be negligible. Once the voltage source is applied, the transient response simulation showed that the potential of the mother subsatellite may again be raised above the neutral plasma potential to a large positive value. Both of these conditions are essential to the success of an electrodynamic mission.

As an example of the use of this tool for planning mission sequence, consider the electroboost mode. An observable change in altitude for the GATE is 15 km. At 2.6 km per day, 6 days of electroboost are required. The necessary stored energy is $480 \times 6 = 2880$ Wh. Conversely, at a 24 Wh per day charging rate, 120 days would pass in the charging mode to replenish the batteries. The electrodynamic model presented clearly demonstrates that the GATE possesses the ability to electrically alter its orbit, either using stored energy for thrust or drawing energy from its orbit for electrical use.

Acknowledgment

This work was supported by Grant NAG 8-618 from the NASA Marshall Space Flight Center, Huntsville, Alabama.

References

- ¹Greene, M., Rupp, C. C., and Lorenzoni, A., "Feasibility Assessment of the Get-Away Tether Experiment," *Advances in the Astronautical Sciences, Tethers in Space*, Vol. 62, American Astronautical Society, San Diego, CA, 1986, pp. 133-142.
- ²Greene, M., "Get-Away Tether Experiment (GATE): A Free Flying Tether Experiment," Final Rept. NAG8-586, Dec. 1986.
- ³Greene, M., Rupp, C. C., Walls, J., Wheelock, D., and Lorenzoni, A., "Feasibility Assessment of the Get-Away Tether Experiment," *Journal of the Astronautical Sciences*, Vol. 35, Jan.-March 1987, pp. 97-118.
- ⁴Dobrowolny, M., "Electrodynamics of Long Metallic Tethers in the Ionospheric Plasma," *Radio Sciences*, Vol. 13, 1978, pp. 417-424.
- ⁵Hastings, D. E., Barnett, A., and Olbert, S., "Radiation from Large Space Structures in Low Earth Orbit with Induced Alternating Currents," *Journal of Geophysical Research*, Vol. 93, 1988, pp. 1945-1960.
- ⁶Barnett, A. and Olbert, S., "Radiation of Plasma Waves by a Conducting Body Moving Through a Magnetized Plasma," *Journal of Geophysical Research*, Vol. 91, 1986, pp. 10117-10135.
- ⁷Arnold, D. A. and Dobrowolny, M., "Transmission Line Model of the Interaction of a Long Metal Wire with the Ionosphere," *Radio Sciences*, Vol. 15, 1980, pp. 1149-1161.
- ⁸Dobrowolny, M., Colombo, G., and Grossi, M. D., "Electrodynamics of Long Tethers in the Near-Earth Environment," *Smithsonian Astrophysical Observatory, Reports in Geoastrophysics*, No. 3, 1976.
- ⁹Belcastro, V., Veltri, P., Dobrowolny, M., "Radiation Resistance of an Infinity Long Tether with Moving Current," *Il Nuovo Cimento*, Vol. 5, 1982, pp. 537-560.
- ¹⁰Dobrowolny, M. and Janve, A. V., "Space Charge Around Conductors at High Potential in Magnetoplasma," *Il Nuovo Cimento*, Vol. 7C, 1984, pp. 292-302.

¹¹Patterson, M. J. and Wilbur, P. J., "Plasma Contactors for Electrodynamic Tether," *Advances in the Astronautical Sciences*, Vol. 62, *Tethers in Space*, American Astronautical Society, San Diego, CA, 1986, pp. 383-406.

¹²Langmuir, I. and Mott-Smith, H. M., "The Theory of Collectors in Gaseous Discharges," *Physical Reviews*, Vol. 28, 1962, pp. 727-763.

¹³Williamson, P. R. and Banks, P. M., "The Tethered Balloon Current Generator—A Space Shuttle-Tethered Subsatellite for Plasma Studies and Power Generation," National Oceanic and Atmospheric Administration Final Report, 1976.

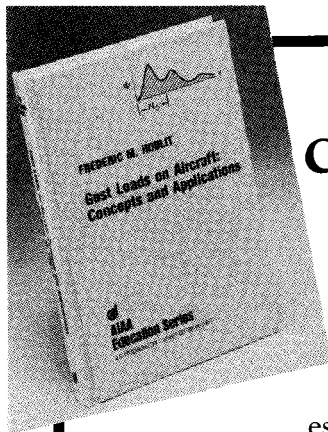
¹⁴Al'pert, Ya. L., Guervich, A. V., and Pitaevskii, L. P., *Space Physics with Artificial Satellites*, Plenum, New York, 1965.

¹⁵Parker, L. W. and Murphy, B. L., "Potential Buildup on an Electron-Emitting Ionospheric Satellite," *Journal of Geophysical Research*, Vol. 72, 1966, pp. 1631-1636.

¹⁶Perkins, F. M., "Flight Mechanics of Low-Thrust Spacecraft," *Journal of the Aerospace Sciences*, Vol. 11, 1959, pp. 291-297.

¹⁷Martinez-Sanchez, M. and Hastings, D. E., "A Systems Study of a 100 KW Electrodynamic Tether," *Advances in the Astronautical Sciences*, Vol. 62, *Tethers in Space*, American Astronautical Society, San Diego, CA, 1986, pp. 341-366.

¹⁸Candidi, M., Dobrowlony, M., and Mariani, F., "The RETE and TEMAG Experiments for the TSS Mission," *Advances in the Astronautical Sciences*, Vol. 62, *Tethers in Space*, American Astronautical Society, San Diego, CA, 1986, pp. 207-216.



Gust Loads on Aircraft: Concepts and Applications by Frederic M. Hoblit

This book contains an authoritative, comprehensive, and practical presentation of the determination of gust loads on airplanes, especially continuous turbulence gust loads.

It emphasizes the basic concepts involved in gust load determination, and enriches the material with discussion of important relationships, definitions of terminology and nomenclature, historical perspective, and explanations of relevant calculations.

A very well written book on the design relation of aircraft to gusts, written by a knowledgeable company engineer with 40 years of practicing experience. Covers the gamut of the gust encounter problem, from atmospheric turbulence modeling to the design of aircraft in response to gusts, and includes coverage of a lot of related statistical treatment and formulae. Good for classroom as well as for practical application...I highly recommend it.

Dr. John C. Houbolt, Chief Scientist
NASA Langley Research Center

To Order, Write, Phone, or FAX:



Order Department

American Institute of Aeronautics and Astronautics
370 L'Enfant Promenade, S.W. ■ Washington, DC 20024-2518
Phone: (202) 646-7444 ■ FAX: (202) 646-7508

AIAA Education Series
1989 308pp. Hardback
ISBN 0-930403-45-2

AIAA Members \$39.95
Nonmembers \$49.95
Order Number: 45-2

Postage and handling \$4.50. Sales tax: CA residents 7%, DC residents 6%. Orders under \$50 must be prepaid. Foreign orders must be prepaid. Please allow 4-6 weeks for delivery. Prices are subject to change without notice.